European Journal of Molecular & Clinical Medicine
ISSN 2515-8260 Volume 08, Issue 02, 2021

A Study Of Covid-19 Spread And Death Contributing Factors In America Using Multi-Layer Perception (MLP) And Radial Basis Function (RBF)

Shafaf IBRAHIM[1], Saadi Ahmad KAMARUDDIN[2], Nur Nabilah ABU MANGSHOR[3], Ahmad Firdaus AHMAD FADZIL[4]

[1,3,4]Faculty of Computer and Mathematical Sciences, Universiti Teknologi MARA, Jasin, Melaka, Malaysia
[2]School of Quantitatives Sciences, College of Arts & Sciences, Universiti Utara Malaysia, 06100 UUM Sintok, Kedah Darul Aman, Malaysia

Abstract: In recent years, Artificial Neural Networks (ANN) was widely implemented for developing predictive and estimation models to estimate the needed parameters. As the Coronavirus disease 2019 (COVID-19) case numbers are rising internationally as uncontrolled outbreaks, it is important to better understand what factors promote the super spreading events. In this paper, the use of Multi-Layer Perceptron (MLP) and Radial Basis Function (RBF) of ANN for COVID-19 spread and death contributing factors in America was described. A comparison was made by using a dataset of COVID-19 cases and deaths reported from 49 states in America during April 2020. Seven covariates used in the network which are High Temperature, Low Temperature, Average Temperature, Population, Percentage of Cases over Population, Percentage of Death over Population, and Total Cases. However, the performance of MLP and RBF networks may be evaluated relatively similar. It was found that both MLP and RBF proved that the Population, Percentage of cases over population, and Total cases are the most contributing factors towards COVID-19 spread and death in America particularly.

Keywords: COVID-19; Contributing factors; Artificial Neural Network (ANN); Multi-layer Perceptron (MLP); Radial Basis Function (RBF)

1. INTRODUCTION

A present worldwide pandemic Coronavirus disease 2019 (COVID-19) is an illness caused by an infectious disease which is severe acute respiratory syndrome coronavirus 2 (SARS-CoV-2) [1]. Approximately 170,000 confirmed cases of COVID-19 have been registered, including an estimated 7,000 deaths in about 150 countries worldwide [2]. A total of 4,226 cases of COVID-19 were reported in the United States as of March 16, with reports drastic rising to 500 or more cases per day starting on March 14. In order to reduce the spread of COVID-19 effectively, it is important to better understand what factors promote the super spreading events [3]. The success of Artificial Neural Networks (ANN) stems mainly from the ability to model not only linear but also non-linear problems effortlessly, and the realistic analysis of issues identified using curvilinear models [1]. The Multilayer Perceptron (MLP) and Radial Basis Function (RBF) networks are the basic classic ANN topologies which widely working as classificatory.

The networks of the MLP were first proposed by [2]-[4]. Numerous successful researches that used the MLP were found [5]-[7]. Among the most studied and most widely used network topologies are one-way multilayer networks of the multilayer perceptron type. On the other hand, the way of RBF networks process information is different. The topology of RBF was proposed by Dave Broomhead and David Lowe [8], [9], as well as John Moody and Christian Darkin [10]. The RBF is a type of feed-forward neural network which uses a supervised training method to learn. It represents a different when compared to sigmoid networks in which the method of mapping the input set into the output file [11], [12]. This transformation consists of matching the function of multivariate approximation to the necessary values. The RBF network typically needs more neurons than one-way networks with the feature of sigmoid activation for construction. Similar to MLP, the RBF network is also widely known for its capabilities in estimation and predication [13], [14].

Considering the great potential of the MLP and RBF, this paper aims to establish a study on MLP and RBF in investigating the contributing factors for COVID-19 spread and death in America. The employment of the ANN is expected to contribute in understanding the contributing factors of the COVID-19 spread and death. The arrangement of the remainder of this paper is as follows: The data background is elaborated in Section 2. Section 3 includes the outlines of our research methods, including the description of MLP and RBF structures. In Section 4, our results are discussed. Finally, we present our conclusion in Section 5.

Data Background

The COVID-19 dataset which includes the number of cases and death were collected from the European Centre for Disease Prevention and Control (ECDPC), global geographical climate data were taken from the Weather Forecast, and population data were obtained from the Current World Population. The descriptive statistics data can be seen in Table 1, and the dataset from cases and deaths reported from 49 states in America is tabulated in Table 2.

Table 1 Descriptive Statistics of Asia

		HIGH TEMP	**LOW TEMP**	**AVG TEMP**	**POPULATION**	**TOTAL CASE**	**TOTAL DEATH**	**% CASES**	**% DEATH**
N	Statistic	49	49	49	49	49	49	49	49
Range	Statistic	65.9	59	58.3	330999171	875288	57796	0.37	0.04
Minimum	Statistic	29.8	19.4	25.3	3480	1	0	0	0
Maximum	Statistic	95.7	78.4	83.6	331002651	875289	57796	0.37	0.04
Sum	Statistic	3875.5	3153.9	3515.3	1021658570	1104863	70905	2.2	0.15
Mean	Statisti	79.09	64.36	71.7	2085017	22548.	1447	0.04	0.00

	c	18	53	408	4.9	2245	.0408	49	31
	Std. Error	2.01773	2.18519	2.04785	8243724.12	17865.79688	1180.74562	0.0105	0.0011
Std. Deviation	Statistic	14.12411	15.29633	14.335	57706068.8	125060.5782	8265.21937	0.0734	0.0074
Variance	Statistic	199.49	233.978	205.492	3.33E+15	15640148209	68313851.3	0.005	0
Skewness	Statistic	-2.217	-1.723	-1.952	4.288	6.882	6.88	2.728	3.908
	Std. Error	0.34	0.34	0.34	0.34	0.34	0.34	0.34	0.34
Kurtosis	Statistic	4.947	2.201	3.185	19.684	47.838	47.808	8.669	16.064
	Std. Error	0.668	0.668	0.668	0.668	0.668	0.668	0.668	0.668

Table 2 America's COVID-19 Cases and Death Data – April 2020

NO	COUNTRY	AVG HIGH TEMP	AVG LOW TEMP	AVG TEMP	POPULATION (2020)	TOTAL CASES	TOTAL DEATH	% CASES/POP	% DEATH/POP
		in °F							
1	Anguilla	82.4	77.0	79.7	15003	1	0	0.0067	0
2	Antigua_and_Barbuda	84.9	74.1	79.5	97929	17	3	0.0174	0.00306
3	Argentina	74.1	56.5	65.3	45195774	3306	190	0.0073	0.00042
4	Aruba	88.7	78.4	83.6	106766	50	2	0.0468	0.00187
5	Bahamas	82.2	66.7	74.5	393244	66	11	0.0168	0.00280
6	Barbados	86.0	75.4	80.7	287375	46	7	0.0160	0.00244
7	Belize	87.8	71.6	79.7	397628	15	2	0.0038	0.00050
8	Bermuda	70.9	62.4	66.7	62278	84	6	0.1349	0.00963
9	Bolivia	62.6	19.4	41.0	11673021	1003	53	0.0086	0.00045
10	Bonaire, Saint	82.4	75.2	78.8	26,223	6	0	0.022	0.0000

	Eustatius and Saba							9	0
11	Brazil	82.0	71.4	76.7	212559417	73583	5307	0.0346	0.00250
12	British_Virgin_Islands	84.2	71.6	77.9	30231	3	1	0.0099	0.00331
13	Canada	52.7	39.4	46.1	37742154	44163	2907	0.1170	0.00770
14	Cayman_Islands	86.0	73.4	79.7	65722	61	0	0.0928	0
15	Chile	73.0	44.4	58.7	19116201	12436	208	0.0651	0.00109
16	Colombia	88.7	76.1	82.4	50882891	5413	264	0.0106	0.00052
17	Costa_Rica	83.1	65.8	74.5	5049118	383	4	0.0075	0.00008
18	Cuba	83.5	69.6	76.6	11326616	1297	54	0.0115	0.00048
19	CuraÃ§ao	88.0	77.9	83.0	164,093	7	0	0.0043	0
20	Dominica	86.0	71.6	78.8	71,986	5	0	0.0070	0
21	Dominican_Republic	83.7	72.5	78.1	10847910	5751	251	0.0530	0.00231
22	Ecuador	69.6	50.4	60.0	17643054	22709	821	0.1287	0.00465
23	El_Salvador	90.0	66.2	78.1	6,486,205	345	9	0.0053	0.00014
24	Falkland_Islands_(Malvinas)	48.0	37.0	42.5	3,480	13	0	0.3736	0
25	Greenland	29.8	20.7	25.3	56770	1	0	0.0018	0
26	Grenada	86.0	77.9	82.0	112523	11	0	0.0098	0
27	Guatemala	82.0	60.8	71.4	17915568	549	15	0.0031	0.00008
28	Guyana	85.1	75.9	80.5	786552	70	7	0.0089	0.00089
29	Haiti	89.6	73.4	81.5	11402528	61	6	0.0005	0.00005
30	Honduras	86.0	69.8	77.9	9,904,607	630	64	0.0064	0.00065
31	Jamaica	86.0	71.6	78.8	2961167	358	6	0.0121	0.00020
32	Mexico	80.2	54.1	67.2	128932753	16705	1704	0.013	0.00132
33	Montserrat	87.8	75.2	81.5	4992	7	2	0.1402	0.04006

34	Nicaragua	93.7	72.7	83.2	6624554	10	3	0.0002	0.00005
35	Panama	95.7	67.1	81.4	4314767	5303	152	0.1229	0.00352
36	Paraguay	83.1	65.5	74.3	7132538	184	6	0.0026	0.00008
37	Peru	75.7	63.7	69.7	32971854	32981	919	0.1000	0.00279
38	Puerto_Rico	30.1	23.6	26.9	2860853	1259	80	0.0440	0.00280
39	Saint_Kitts_and_Nevis	84.2	73.4	78.8	53199	8	0	0.0150	0
40	Saint_Lucia	84.2	73.4	78.8	183627	8	0	0.0046	0
41	Saint_Vincent_and_the_Grenadines	84.2	71.6	77.9	110940	15	0	0.01352	0
42	Sint_Maarten	86.0	75.2	80.6	42876	73	13	0.1703	0.03032
43	Suriname	87.8	71.6	79.7	586632	2	1	0.0003	0.00017
44	Trinidad_and_Tobago	86.0	73.4	79.7	1399488	31	5	0.0022	0.00036
45	Turks_and_Caicos_islands	84.2	71.6	77.9	38717	7	1	0.0181	0.00258
46	United_States_of_America	55.0	37.0	46.0	331002651	875289	57796	0.2644	0.01746
47	United_States_Virgin_Islands	84.0	72.0	78.0	104425	36	4	0.0345	0.00383
48	Uruguay	71.6	55.2	63.4	3473730	306	14	0.0088	0.00040
49	Venezuela	77.0	63.5	70.3	28435940	196	7	0.0007	0.00002

2. RESEARCH METHODS

This paper aims to establish a study on COVID-19 spread and death contributing factors in America using MLP and RBF. Seven covariates used in the network which are High Temperature, Low Temperature, Average Temperature, Population, Percentage of Cases over Population, Percentage of Death over Population, and Total Cases. These seven covariates were the inputs nodes in the input layer of the network. The description of the MLP and RBF structures are explained further in the next subsections.

Multilayer Perceptron (MLP) Network

The MLP is a class of feed forward network and is considered as the most utilized model for back-propagation neural network training [15]. It employs multiple layers which include input, multiple hidden layers, and an output layer [16]. This network has been demonstrated to be applicable in various fields of studies such as prediction [17], [18] and classification [19]. Figure 1 illustrates a basic MLP network with two hidden layers.

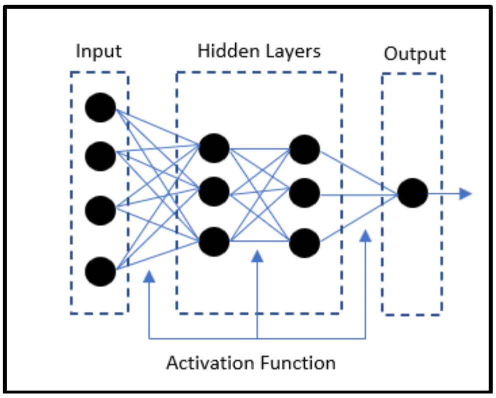

Figure 1 MLP Network Example

The input is assigned with appropriate weights that will be carried over to the hidden layers. In each hidden layer, an activation function will be employed to generate relationships between input and output vectors. Equation (1) represents the appropriate mathematical expression of MLP.

$$a = f\ (w_i + b) \tag{1}$$

where:
a: output signal of the neuron
w: weights between the neurons
i: vector of input data
b: bias added to the neurons where each neuron in the network includes an activation function (*f*)

The examples of popular MLP activation functions include thresholding, hyperbolic tangent, gaussian, and stochastic [20]. The output layer will acquire the result from previous layer to produce the target output of the network [21]. Conventionally, the activation function to produce the output in MLP network is sigmoid function before linearly combine the output generated from previous layer [22]. In this study, the MLP network consists of four hidden layer, with one single node. The activation function from input layer to hidden layer was Hyperbolic tangent. The target of the network is COVID-19 spread and death, where the activation function from hidden layer to output layer was identity (purelin). The default error function in backpropagation neural network was based on sum of squares (SSE). To simplify, the configurations of this network was 7-4-1. The network architecture for MLP can be referred in Figure 2.

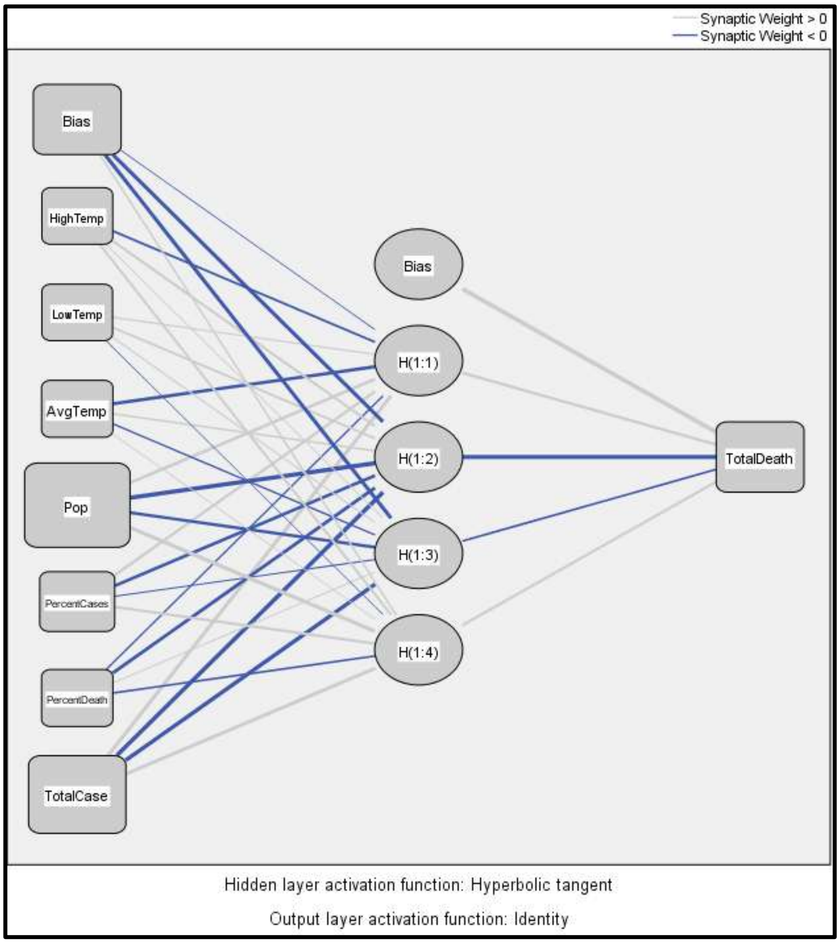

Figure 2 MLP network architecture

Radial Basis Function (RBF) Network

The RBF network is a simpler approach compared to the MLP network. This model consists of three layers of network which are input, hidden, and output [23]. Similar to MLP, RBF network is also demonstrated to be successfully employed in field of studies such as prediction [24], [25] and classification [26]. This suggests that both MLP and RBF cater towards similar problems despite being considerably different in terms of the technique employed. RBF Network is configured with only one hidden layer while MLP is usually configured with more. The example of RBF neural network is depicted in Figure 3.

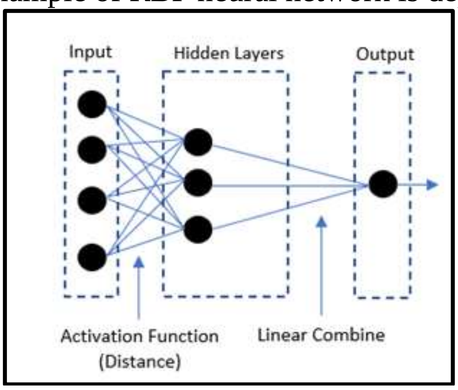

Figure 3 RBF Network Example

The networks neuron which is the RBF activation function is located in the hidden layer. Radial functions are a special class of functions the value of which increases or decreases proportional to the distance from a central point. The formulation of a RBF output is as Equation (2):

$$y_i(x) = \sum_{j=1}^{k} w_{ij}\, \phi(\|x - c_j\|) \tag{2}$$

where:
x = input vector
y_i = network's ith output
K = number of neurons in the hidden layer
C_j = center of the jth hidden neuron
w_{ij} = weight of the link from the jth neuron in the hidden layer to the ith neuron in the output layer
$\|.\|$ = Euclidian norm
ϕ = RBF which is used in the neurons of hidden layer

There are various types of RBF, but Gaussian function is the most employed [27] which is defined as Equation (3):

$$\phi(\|x - c_j\|) = e^{\left(-\frac{\|x-c_j\|^2}{2\sigma_j^2}\right)} \tag{3}$$

The σ_j is the width of the jth hidden neuron. While MLP employed activation function before linearly combine to produce the output in the final layer, RBF take the results from the previous layer and perform linear combination without employing any activation function. The weighted sum of every RBF neuron output is carried over towards the output layer neurons to decide the final output [28].

On the contrary to the MLP, the RBF consists of only one hidden layer, with one single node. The activation function from input layer to hidden layer was Softmax. Similar to the MLP, the target of the network is COVID-19 spread and death, where the activation function from hidden layer to output layer was identity (purelin). The default error function in backpropagation neural network was based on SSE. To simplify, the configurations of this network was 7-1-1. The network architecture for RBF is illustrated in Figure 4.

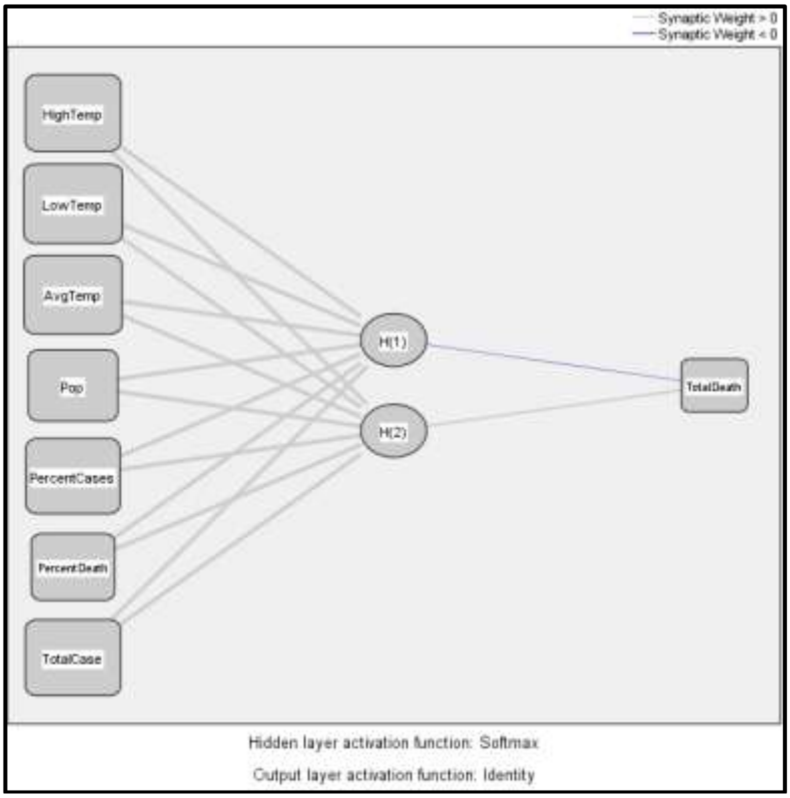

Figure 4 RBF network architecture

3. RESULTS AND DISCUSSION

The case processing summary for MLP and RBF are presented in Table 3 and Table 4 respectively. The data were divided into two sets which are training and testing. Based on the Table 3, the training set for MLP consist of 77.6% (38/49) of the overall data, while testing sets comprises of 22.4% (11/49) of the overall data, N=49. There were no excluded values recorded.

Table 3 MLP Case Processing Summary

		N	**Percent**
Sample	Training	38	77.6%
	Testing	11	22.4%
Valid		49	100.0%
Excluded		0	
Total		49	

The training set for RBF in contrast consist of 69.4% (34/49) of the overall data, while testing sets comprises of 30.6% (15/49) of the overall data, N=49. There were no excluded values recorded as well as depicted in Table 4.

Table 4 RBF Case Processing Summary

	N	**Percent**

Sample	Training	34	69.4%
	Testing	15	30.6%
Valid		49	100.0%
Excluded		0	
Total		49	

Table 5 tabulates the independent variable importance for MLP network. Referring to Table 5, the MLP network concluded that the Population contributes to the highest contributing factor towards COVID-19 spread and death which is 100% of normalized importance. It is followed by the Total cases (76.8%) and Percentage of cases over population (13.1%). It is monitored that the climate which referring to high temperature, low temperature, and average temperature are seem to not really contribute to COVID-19 spread and death as they only returned little percentage of normalized importance which are HighTemp (1.5%), LowTemp (1.1%), and AvgTemp (2.8%). The graph of the MLP independent variable importance is presented in Figure 5.

Table 5 MLP Independent Variable Importance

	Importance	**Normalized Importance**
HighTemp	.008	1.5%
LowTemp	.005	1.1%
AvgTemp	.014	2.8%
Population	.505	100.0%
PercentCases	.066	13.1%
PercentDeath	.014	2.7%
TotalCase	.388	76.8%

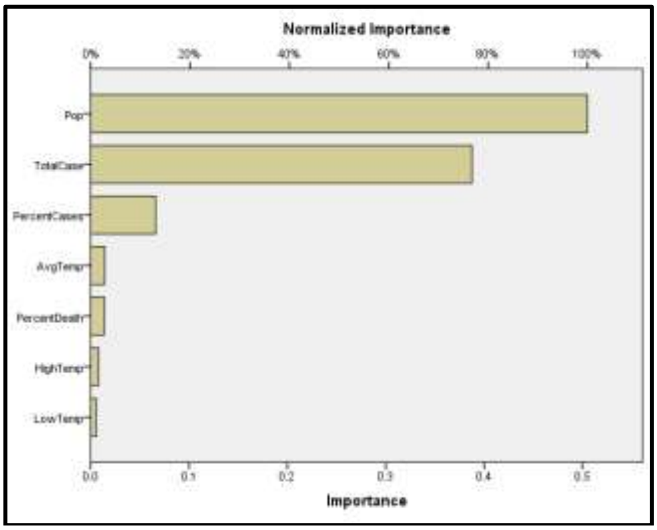

Figure 5 MLP independent variable importance graph

The RBF network similarly determined that the most important contributing factors towards COVID-19 spread and death are the Population (100%), Percentage of cases over population (34.1%), and Total cases (33.7%) as shown in Table 6 and Figure 6.

Table 6 RBF Independent Variable Importance

	Importance	**Normalized Importance**
HighTemp	.037	7.5%
LowTemp	.045	9.2%
AvgTemp	.041	8.4%
Population	.489	100.0%
PercentCases	.167	34.1%
PercentDeath	.057	11.7%
TotalCase	.165	33.7%

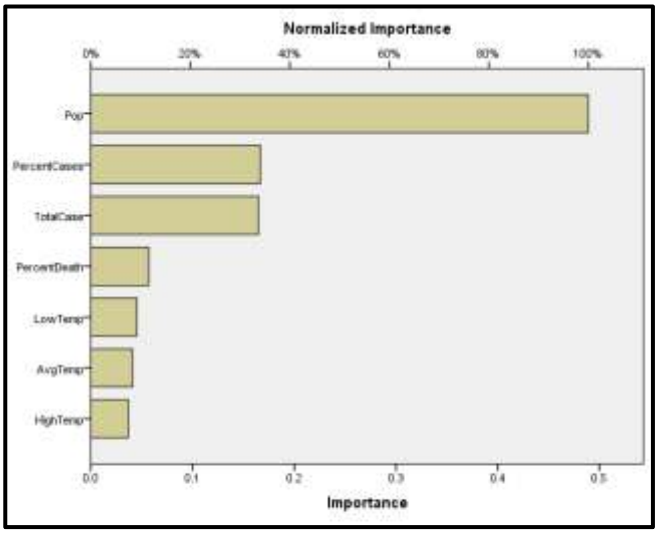

Figure 6 RBF independent variable importance graph

The performance of the developed MLP and RBF networks were then evaluated and investigated against an empirical correlation using statistical and graphical error analyses which are Sum of Squared Error (SSE) and Relative Error (RE). The method of rescaling covariates is Standardized by nature. In this rescaling process, mean is subtracted from the values and the outcome is divided by the standard deviation. There are three more methods of rescaling which are Normalized, Adjusted normalized and None. The MLP network comprises of two optimization algorithms which are Scaled Conjugate Gradient and Gradient Descent. In comparison, the Normalized Radial Basis Function (NRBF) and Ordinary Radial Basis Function (ORBF) are used to represent the RBF. Table 7, Table 8, Table 9 and Table 10 demonstrate the overall summary of RE and SSE for both MLP and RBF correspondingly.

Table 7 RE of ANN MLP Models

Rescaling of Covariates	**Optimization Algorithm**	
	Scaled Conjugate Gradient	**Gradient Descent**

Standardized	0.033	0.001
Normalized	0.061	0.002
Adjusted Normalized	0.010	1.057
None	1.014	1.009

Table 8 SSE of ANN MLP Models

Rescaling of Covariates	**Optimization Algorithm**	
	Scaled Conjugate Gradient	**Gradient Descent**
Standardized	0.590	0.018
Normalized	0.769	0.030
Adjusted Normalized	0.180	19.561
None	16.735	17.661

Based on the Table 7 and Table 8, it can be monitored that MLP produced the best result in Adjusted Standardized rescaling method (Scaled Conjugate Gradient), in which it returned the lowest values of RE and SSE of 0.010 and 0.180 as compared to the Normalized, Adjusted Normalized, and None. The Gradient Descent however produced the lowest values of RE and SSE in the Standardized method which are 0.001 (RE) and 0.018 (SSE) as compared to the ORBF. Instead, the RBF is seen to compute the lowest RE and SSE values in the Normalized rescaling method which are 0.001and 0.014 (NRBF), and are found to produce lower error rates than the MLP network as shown in Table 9 and Table 10. The OBRF in some way returned the lowest RE and SSE in the None rescaling covariates which are 0.002 (RE) and 0.043 (SSE).

Table 9 RE of ANN RBF Models

Rescaling of Covariates	**Radial Basis Neural Network Activation Function for Hidden Layer**	
	Normalized Radial Basis Function	**Ordinary Radial Basis Function**
Standardized	0.003	0.826
Normalized	0.001	0.766
Adjusted Normalized	0.812	0.008
None	0.008	0.002

Table 10: SSE of ANN RBF Models

Rescaling of Covariates	**Radial Basis Neural Network Activation Function for Hidden Layer**	
	Normalized Radial Basis Function	**Ordinary Radial Basis Function**
Standardized	0.047	13.637
Normalized	0.014	14.942
Adjusted Normalized	11.372	0.124
None	0.13	0.043

The testing set should be the reference in any network. The performance of MLP and RBF networks may be evaluated relatively similar. The RE values for both MLP and RBF are monitored to be quite low. Therefore, it is firmly believed that both MLP and RBF network performances are in favorable structure. All configurations of both techniques can be referred in Table 11 and Table 12.

Table 11 Configurations of ANN MLP Models

Rescaling of Covariates	Optimization Algorithm	
	Scaled Conjugate Gradient	**Gradient Descent**
Standardized	7-2-1	7-3-1
Normalized	7-2-1	7-1-1
Adjusted Normalized	7-4-1	7-4-1
None	7-5-1	7-4-1

Table 12 Configurations of ANN RBF Models

Rescaling of Covariates	Radial Basis Neural Network Activation Function for Hidden Layer	
	Normalized Radial Basis Function	**Ordinary Radial Basis Function**
Standardized	7-9-1	7-1-1
Normalized	7-10-1	7-1-1
Adjusted Normalized	7-2-1	7-3-1
None	7-3-1	7-5-1

In a nutshell, the performance evaluation indicated that both ANN models of MLP and RBF are effective in investigating the contributing factors of COVID-19 spread and death. From the testing conducted, it is found the climate does not strongly contribute to COVID-19 spread and death. It could also be concluded that the Population, Percentage of cases over population, and Total cases are the most contributing factors towards COVID-19 spread and death in America particularly.

4. CONCLUSIONS

This paper presents a study of COVID-19 spread and death contributing factors in America using Multi-Layer Perceptron (MLP) and Radial Basis Function (RBF). A comparison was made by using a dataset of COVID-19 cases in 49 America states during April 2020. There are seven contributing factors which acted as the covariates to the network such as High Temperature, Low Temperature, Average Temperature, Population, Percentage of Cases over Population, Percentage of Death over Population, and Total Cases. The performance evaluation indicated that both ANN models of MLP and RBF are effective in investigating the contributing factors of COVID-19 spread and death. From the testing conducted, both MLP and RBF proved that the Population, Percentage of cases over population, and Total cases are the most contributing factors towards COVID-19 spread and death in America particularly.

Acknowledgements

The research was supported by Universiti Teknologi MARA Cawangan Melaka through the Teja Internal Grant 2020 (GDT2020-19).

REFERENCES

[1] P Boniecki, M Zaborowicz, A Pilarska and H Piekarska-Boniecka. Identification Process of Selected Graphic Features Apple Tree Pests by Neural Models Type MLP, RBF and DNN. *Agriculture 2020*. 2020; **10**, 218.

[2] D Li, R Wang, C Xie, L Liu, J Zhang, R Li, F Wang, M Zhou and WA Liu. Recognition Method for Rice Plant Diseases and Pests Video Detection Based on Deep Convolutional Neural Network. *Sensors 2020*. 2020; **20**, 578.

[3] P Boniecki, K Nowakowski and RL Tomczak. *Neural networks type MLP in the process of identification chosen varieties of maize*. In Proceedings of the 3rd International Conference on Digital Image Processing (ICDIP 2011), SPIE Proceedings, Chengdu, China, 2011, **8009**, 15-17.

[4] A Pilarska, K Pilarski, K Witaszek, H Waliszewska, M Zborowska, B Waliszewska, M Kolasi ´nski and K Szwarc-Rzepka. Treatment of dairy waste by anaerobic co-digestion with sewage sludge. *Ecol. Chem. Eng*. 2016; **23**, p 99-115.

[5] S Amid and T Mesri Gundoshmian. Prediction of output energies for broiler production using linear regression, ANN (MLP, RBF), and ANFIS models. *Environ. Prog. Sustainable Energy*. 2017; **36**, p 577-585.

[6] KG Harish and KP Radha. Investigation of thermal performance of unidirectional flow porous bed solar air heater using MLP, GRNN, and RBF models of ANN technique. *Thermal Science and Engineering Progress*. 2018; **6**, p 226-235.

[7] A Mahdi, BZ Amin, N Zahra and Z Zhien. Prediction of solubility of N-alkanes in supercritical CO2 using RBF-ANN and MLP-ANN. *Journal of CO2 Utilization*. 2018; **25**, 108-119.

[8] P Boniecki, K Koszela, K Swierczy´nski, J Skwarcz, M Zaborowicz and J Przybył. Neural Visual Detection of Grain Weevil (Sitophilus granarius L.). *Agriculture 2020*. 2020; **10**, 25.

[9] P Boniecki, K Koszela, H Piekarska-Boniecka, K Nowakowski, J Przybył, M Zaborowicz, B Raba and J Dach. *Identification of selected apple pests, based on selected graphical parameters*. In Proceedings of the 5th International Conference on Digital Image Processing, Proceedings of SPIE, Beijing, China. 2013, 8878.

[10] P Boniecki, K Nowakowski, P Slósarz, J Dach and K Pilarski. *Neural image analysis for estimating aerobic and anaerobic decomposition of organic matter based on the example of straw decomposition.* In Proceedings of the 4th International Conference on Digital Image Processing, Proceedings of SPIE, Kuala Lumpur, Malaysia, 2012, 8334.

[11] K Nowakowski, P Boniecki and J Dach. *The Identification of Mechanical Damages of Kernels Basis on Neural Image Analysis*. In Proceedings of the International Conference on Digital Image Processing (ICDIP 2009). Bangkok, Thailand, 2009, p 412-414.

[12] S Kujawa, RJ Tomczak, T Kluza, J Weres and P Boniecki. *A stand for the image acquisition of composted material based on the sewage sludge.* In Proceedings of the

4th International Conference on Digital Image Processing (ICDIP 2012), Proceedings of SPIE, Kuala Lumpur, Malaysia, 2012, 83341R.

[13] E Asnaashari, M Asnaashari, A Ehtiati et al. Comparison of adaptive neuro-fuzzy inference system and artificial neural networks (MLP and RBF) for estimation of oxidation parameters of soybean oil added with curcumin. *Journal of Food Measurement and Characterization*. 2015; **9**, 215-224.

[14] M Moosavi, K Firoozi Rad and A Daneshvar. A comparative study in the prediction of thermal conductivity enhancement of nanofluids using ANN-MLP, ANN-RBF, ANFIS, and GMDH methods. *J Iran Chem Soc*. 2019; **16**, 2629-2637.

[15] H Ramchoun, MAJ Idrissi, Y Ghanou and M Ettaouil. Multilayer Perceptron: Architecture Optimization and Training. *IJIMAI*. 2016; **4**(1), 26-30.

[16] K Kwon, D Kim and H Park. Parallel MR imaging method using multilayer perceptron. *Medical physics*. 2017; **44(12)**, 6209-6224.

[17] Z Ali, I Hussain, M Faisal, HM Nazir, T Hussain, MY Shad, GS Hussain. Forecasting drought using multilayer perceptron artificial neural network model. *Advances in Meteorology*. **2017**; 1-9.

[18] E Heidari, MA Sobati and S Movahedirad. Accurate prediction of nanofluid viscosity using a multilayer perceptron artificial neural network (MLP-ANN). *Chemometrics and intelligent laboratory systems*. 2016; **155**, 73-85.

[19] P Naraei, A Abhari and A Sadeghian. *Application of multilayer perceptron neural networks and support vector machines in classification of healthcare data*. In 2016 Future Technologies Conference (FTC). 2016, p 848-852.

[20] IS Isa, Z Saad, S Omar, MK Osman, KA Ahmad and HM Sakim. *Suitable MLP network activation functions for breast cancer and thyroid disease detection*. In 2010 Second International Conference on Computational Intelligence, Modelling and Simulation. 2010, p 39-44.

[21] Y Zhang, Y Sun, P Phillips, G Liu, X Zhou and S Wang. A multilayer perceptron based smart pathological brain detection system by fractional Fourier entropy. *Journal of medical systems*. 2016; **40(7)**, 173.

[22] MA Ghorbani, HA Zadeh, M Isazadeh and O Terzi. A comparative study of artificial neural network (MLP, RBF) and support vector machine models for river flow prediction. *Environmental Earth Sciences*. 2016; **75(6)**, 476.

[23] Y Li, X Wang, S Sun, X Ma and G Lu. Forecasting short-term subway passenger flow under special events scenarios using multiscale radial basis function networks. *Transportation Research Part C: Emerging Technologies*, 2017; **77**, 306-328.

[24] YY Ou..Prediction of FAD binding sites in electron transport proteins according to efficient radial basis function networks and significant amino acid pairs. *BMC bioinformatics*. 2016; **17(1)**, 298.

[25] P Hartono. Classification and dimensional reduction using restricted radial basis function networks. *Neural Computing and Applications*. 2018; **30(3)**, 905-915.

[26] I Aljarah, H Faris, S Mirjalili and N Al-Madi. Training radial basis function networks using biogeography-based optimizer. *Neural Computing and Applications*. 2018; **29(7)**, 529-553.